Preface

An estimated 19 million people have limited mobility resulting from some form of neuromuscular dysfunction and/or degenerative diseases [1]. These diseases are often incurable, but assistive devices actuated with artificial muscles can be used to restore function and quality of life. Current artificial muscles include but are not limited to: shape memory alloys (SMAs), pneumatic artificial muscles (PAMs), electroactive polymers (EAPs), and thermal actuators [2,3]. Each of these aforementioned muscles are limited by their functionality, cost, size, and/or biocompatiblity. Mandrel formed Twisted Coiled Polymer (TCP) muscles are an existing, but under researched form of thermally actuated artificial muscles, which are made by coiling a highly twisted monofilament plastics such as Nylon 6/6 (sewing thread) helically [4]. An increase in temperature causes the fiber to shrink axially and expand radially. The radial expansion causes fiber untwisting, which results in a larger tensile contraction (TC) and tensile stress (TS), than that of untwisted fibers. To cause expansions, TCP muscles can also be coiled in the opposite direction of their fiber twist. These heterochiral fibers can be used to counteract length changes of the homochiral muscles caused by ambient temperature changes. Currently mandrel formed TCP muscles require a 70 °C temperature change to be comparable with human muscle, which have an average TS of 0.35 MPa and TC greater than 40% [2,3,4]. This temperature change is highly restrictive for applications of these muscles within the human body or as passively actuated assistive devices. If the amount of contraction was significantly increased and the tensile stress exerted remained above that of human muscle the TCP muscles could be comparable to human muscles at much lower temperature ranges.

Table of Contents

Table of Figures

Introduction

Twisted Coiled Polymer (TCP) Muscles have demonstrated their ability to surpass human muscle. Currently, the maximum contraction of 49% initial length for mandrel formed TCP muscles has taken place at a 5.1 spring index and has achieved a 1 MPa stress over a 70 °C temperature range (25°C to 95°C) [4]. Several groups have even used TCP muscles for proof of concept prosthetic limb applications [5,6,7,8,9]. In order to make viable TCP muscles that actuate over body temperature range of (33.2 °C to 38.2 °C), the contraction must be improved by 1143% to have a 40% TC, but the stress can be reduced by 65% to have a viable TS of 0.35 MPa.

Human skeletal muscles, as stated before, have a maximum Tensile Stress (TS) of 0.35 MPa and Tensile Contraction (TC) of greater than 40% its initial length [2,3]. For a class of artificial muscle to be considered a viable replacement for human muscle it has to have comparable TS and TC to that of the best human skeletal muscle. In order for a material to be implantable, it has to be nontoxic, nondegradable, bioinert, and must be able to withstand all possible stresses of the human body without deforming plastically or injuring surrounding tissues. The Nylon 6, Nylon 6/6, and polyethylene terephthalate (PET) are known biomaterials already approved for applications within the human body [10,11].

The primary aim of this study was to determine if a TCP muscle could exert a 0.35 MPa stress while contracting 40% its initial length over the full range of human body temperature. To validate these aspects, an isotonic test is proposed. This isotonic testing chamber heats the TCP muscles from 33.2 °C to 38.2 °C while they are tensioned by a 1.75g weight. This experiment determines if the muscle made from 0.25 mm diameter monofilament can contract 40% its length while exerting

a stress of 0.35 MPa. An isometric analysis of the TCP muscles is also intended. In this analysis the fiber's length does not change and the maximum force is measured. This secondary test would determine the maximal force these muscles can exert and if the muscle fails catastrophically when it actuates against an immovable object. After both the isotonic and isometric tests are done, a fatigue test is intended to determine the life span of these viable TCP muscles. These factors are crucial for determining the utility of TCP muscles in prosthetic and biomaterial applications, but were not able to be measured during the course of this research.

Before the aims of **isotonic muscle validation** and **isometric muscle verification** could be accomplished, manufacturing methodologies were formulated and monomer characteristics that affect twist insertion were quantified. A consistent methodology for manufacturing precursor TCP muscles was created utilizing equipment designed for fishing line. The primary factors that had to be determined were the material properties of each monomer. Once these were determined, twist insertion could be optimized, as the amount of fiber untwist has been proposed as the largest contributing factor responsible for the length changes of TCP muscles [12].

The specific amount of twists/m was hypothesized to depend on the specific monofilament's shear modulus, elastic modulus, tensile stress, and diameter [13,14]. As this was not the main aim of the paper the fiber was stressed to 75% of its maximum during twist insertion, because no fibers tensioned at this stress broke during the materials analysis and prior literature proposed the maximum twist/m for a fiber increased with stress. However, this twisting methodology caused the fiber to break at a twist/m value that was an order of magnitude less than that predicted using the equations proposed in prior literature. It was then determined that the relation of twist insertion

to tensile stress must be fully evaluated before moving forward, as the TC of these muscles could not be improved the amount required without this step.

Throughout this research, several discoveries were made about the manufacturing requirements of TCP muscles. Some insight was gained as to the manufacturing parameters which optimize the TCP muscle geometries based on specific requirements of temperature, TS, and TC. Despite these novel findings, consistent manufacturing and analysis of several unique TCP muscle coil geometries was not accomplished due to several setbacks, unforeseen additional experiments, and the highly difficult machine design and fabrication process. In other words, the overarching hypothesis, large diameter coils with small bias angles made of highly twisted fibers will contract more than small diameter coils with large bias angles made of highly twisted fibers, could not be tested and no ideal combination of coil diameter or coil bias angle could be determined to cause a contraction of 40% initial length in a 5 °C temperature range.

Materials and Methods

Monomer Selection

Previous literature indicates that fibers of small diameter, low shear modulus, high elastic modulus, high ultimate stress and a large anisotropic thermal expansion coefficient would be ideal for making TCP muscles of large TC. As a secondary design consideration, we desired a low cost, commonly available, and biocompatible monomer that was approved for existing biomedical applications. Several polymers were considered for this including Low Density Polyethylene, High Density Polyethylene, Nylon 6,6, Nylon 6, Polyethylene Terephthalate (PET), Acrylonitrile Butadiene Styrene (ABS), Polytetrafluoroethylene (PTFE), Polyglycolic Acid (PGA), and Polylactic Acid (PLA). PET is hypothesized, based on equations proposed in prior research, to be the ideal "non-biodegradable" monomer for TC [12,13]. Nylon 6 was hypothesized to be and intermediate monomer for TC and TS. Nylon 6,6 is hypothesized to be the best TS monomer. PGA is hypothesized to be the best biodegradable monomer for TC and TS. With all this in mind PET and Nylon 6 were obtained. The PET selected for this experiment was 0.25mm diameter PET Type 1 from TORAY MONOFILAMENT CO., LTD. However, from that same supplier PET Type 2 was the only filament available at 0.25mm and the Type 1 filament at 0.75mm, from a rudimentary compliance test, was determined to be less advantageous for twist insertion than the Type 2 fiber, as it sheared easily and required a large tensile force. For the 0.25mm Nylon 6 monomer the FISHINGSIR® MonoPro Monofilament Fishing Lines Premium Mono Nylon Material is selected. No PGA was acquired as it is not a commonly available polymer and is readily biodegradable.

Tension Testing

Tension testing was done to determine the relationship of stress and strain for the 0.25mm samples of Nylon 6 and PET. The elastic modulus or the slope of a stress-strain curve and the maximum stress are all needed to properly evaluate the twist/m equations mentioned in the introduction. To maintain consistency between tests, 22in samples of each filament were cut. Before each sample was added to the tension testing machine the distance between the coupon fixtures was adjusted to approximately 10cm. When fixed to the tension testing machine, each sample was clamped in the top flat coupon fixture, wrapped around the top nut three times strung to the bottom nut where it was wrapped three more times the opposite direction, and then clamped in the bottom flat coupon fixture as seen in Figure 1. The tension testing machine was a PASCO Materials Testing Machine ME-8236, which can be seen in Fig. 2. While this materials testing machine was sufficient for this experiment, in an ideal stress-strain experiment maintains a slow, constant loading rate.

Figure 1. Tension Testing Setup. A picture of the 0.25mm Nylon 6 being placed in the tension testing machine

Figure 2. PASCO Materials Testing Machine ME-8236. A Pictures of the PASCO Materials Testing Machine ME-8236 taken by the experimenter

Precursor TCP Muscle Manufacturing

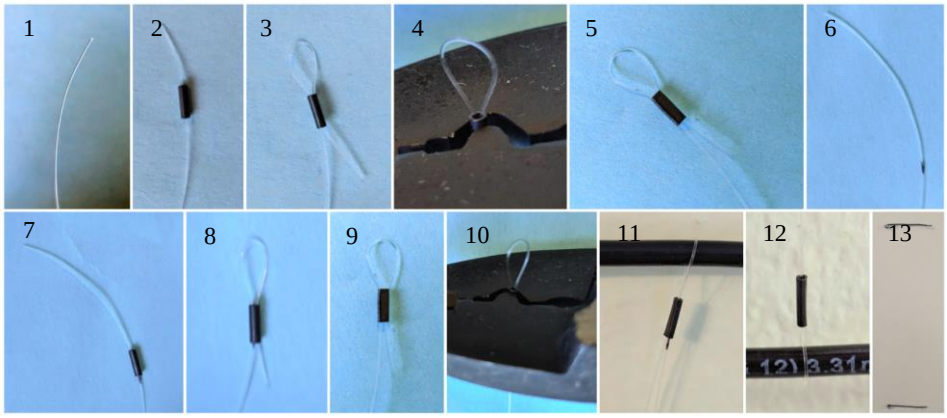

Figure 3. Manufacturing Methodology of a Precursor TCP Muscle. Steps required to make a precursor TCP muscle or fiber sample

The consistent tensile and torsional properties of the monomer samples are paramount for producing consistent results. To produce a consistent sample requires 13 steps.

Step 1: Remove fiber from the spool

Step 2: Feed fiber through an American Fishing Wire Single Barrel Crimp Sleeve

Step 3: Feed the fiber back through to make a loop

Step 4: Crimp the fiber with a crimping tool

Step 5: Tug on the fiber to make sure it is secured in the crimp

Step 6: Measure out the length between the crimps with another sample of desired length, marking it, and cutting the fiber at a reasonable distance away from the mark.

Step 7: Feed the crimp onto the fiber, so that it covers the mark

Step 8: Feed fiber through a crimp

Step 9: Feed the fiber back through to make a loop

Step 10: Crimp the fiber with a crimping tool

Step 11: Tug on the fiber to make sure it is secured in the crimp and hang it on a section of wire

Step 12: Attach the fiber to lower section of wire

Step 13: Repeat steps 1-12 until you have a significant sample size

The variability in eyelet size was noted to create error in the amount of twists inserted into the fiber by around 10-20 turns, as the loop twisted until it had no remaining room area in the eyelet and then the fiber started to twist. During sample storing it was determined that having the fibers fixed only on one end allowed the fibers to get tangled, but fixing the fibers at both ends prevented them from interacting with one another. The crimping tool is necessary in this setup as needle nose pliers apply pressure unevenly and inconsistently, which increases error in the twisting experiment. Ultimately the fiber sample manufacturing methodology proposed in this paper is more consistent, more time efficient, and is better for fiber integrity than any knot.

Twist Insertion

Once the twisting machine (Fig. 4) was I determined the acrylic density using the volume defined in the SolidWorks assembly. I then weighed it and myself simultaneously and then subtracted (tared) my bodyweight. The density of ¼" thick acrylic was determined to be 1.02

g/cm^3. While the acrylic sheets were not exactly ¼" thick as designed and there was variance in thickness, this rudimentary density analysis was sufficient for determining what dimensions of acrylic should be cut to make weights of specific mass.

These acrylic weights are used to fix the fibers axially under a 100 rpm micro gear motor and to tension them vertically. The precursor TCP muscle is connect to the gear motor and the weight by hooks made from 12 gauge copper. The 100 rpm micro gear motor has an rpm counter and is controlled/monitored by an Arduino Mega. The number of twists is displayed on a 16x2 serial enabled Liquid Crystal Display (LCD).

The acrylic guide weights prevent the bottom of the fiber from rotating, while allowing the weight to move upward. Each of these guide weights has four ¼" diameter holes in them used for hanging weights and attaching the wire hook used for tensioning the fiber. The volume of these ¼" diameter holes and mass of the wire hooks was accounted for when determining the weight dimensions needed to create a specific mass. The weight masses were tailored to range from 60% the maximum stress to below 7% maximum stress. To accomplish this two acrylic weights were cut for each monomer.

The two weights for each monomer differed by 250g, so that the experimenter could add and subtract mass with 500g, 1000g, and 1500g weights while maintaining the 250g resolution. Many of these stresses cause a fiber length of 0.5m to stretch to the point where the weights are in contact with the bed of the twisting machine; for this reason 0.25m of fiber is used to determine the twist/m unique to each monomer at each stress. At this point, I thought a method

of hand coiling would be possible and could form coils consistently; however, this opinion changed drastically as several more rudimentary methods were tested.

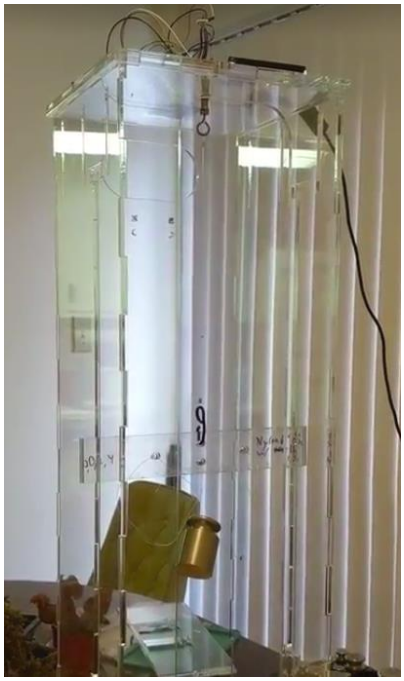

Figure 4. Twisting Machine. A picture of the twisting machine designed and assembled for this exeriment in use. The acrylic guide weight prevents the bottom of the fiber from rotating axially. The weight of the acrylic guide was incremented in this picture by a 1 kg weight. The 110 rpm motor at the top twists the fiber and its rpm counter determines the number of revolutions it has done

Mandrel Coiling

The methods attempted that did not succeed include lathing a grove in the mandrel for a fiber to sit while simultaneously functioning as a lead screw in a linear actuator, having a nut and bolt of

specific bias angles that could be fixed to the mandrels regardless of diameter, and following a guide line drawn on the mandrel. The leadscrew idea was not feasible for smaller diameter mandrels as a lath's cutting tool would deflect the mandrel before cutting it. The nut and bolt idea was not feasible as the diameter of the mandrel determines the turns/m possible, meaning different mandrel diameters would have had different bias angles and the consistency of the samples would be compromised. The last concept was not feasible as it would be very time consuming and inaccurate to do this experiment by hand.

For this research, a custom coiling device was designed to twist and coil fibers up to a half a meter of length around mandrel diameters from the 1/64" up to 1". On the coiling machine, three 4900 rpm dc micro gear motors each rotate a Traxxas 3945 15-T gear that meshes with the chuck's 20-T laser cut acrylic gear which rotates the mandrel. Two 90 rpm dc micro gear motors each rotate a Traxxas 3945 15-T pinion gear along a 124-T 12" acrylic laser cut rack to move the chuck linearly away from the twisting machine. The chuck and its motors can be seen in Figure 5 and the complete coiling machine integrated into the twisting machine can be seen in Figure 6.

The control interface of the TCP Machine consists of a button to initiate and end twisting, a button to switch between twisting and coiling, a button to select the desired bias angle, a button to select the desired mandrel diameter, a button to imitate coiling, and an LCD screen that issues commands and requests input. This LCD screen is the same screen used by the twisting machine. An Arduino Mega was necessary as an Arduino Uno does not have enough interruptible pins to both display on an LCD and monitor three separate motor rpms.

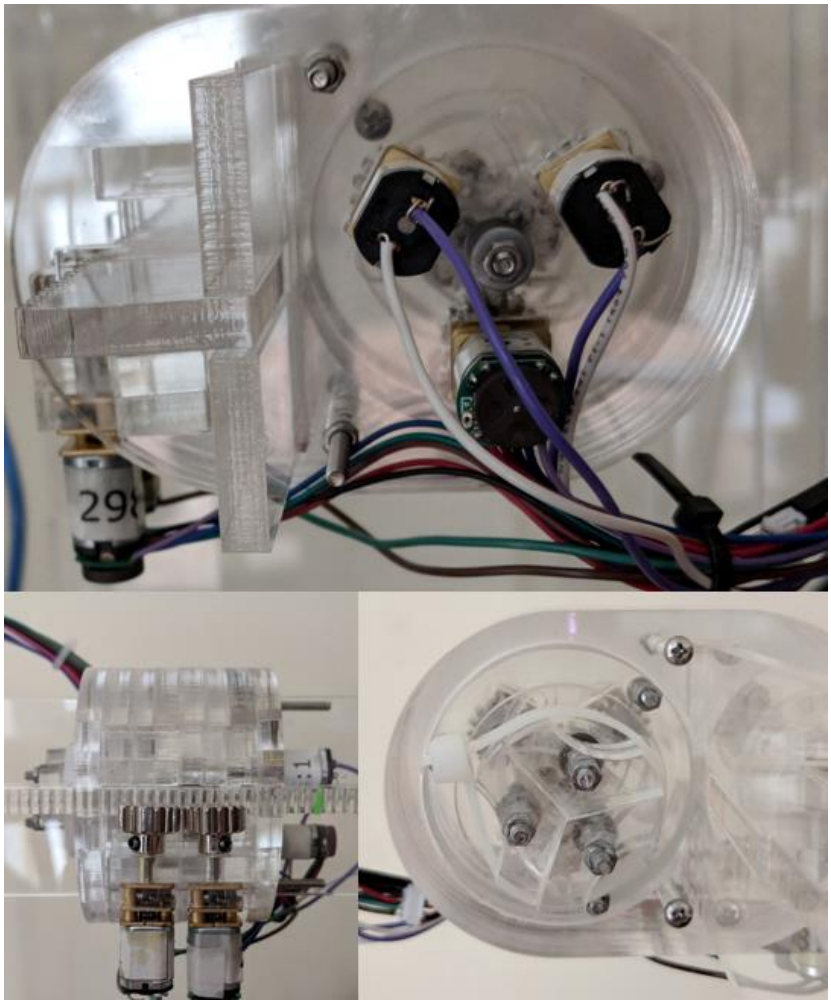

Figure 5. Chuck and Pinion Motors. The chuck and pinion motors of the coiling machine. The bite of the chuck allows for mandrel diameters the size of a human hair up to 1”

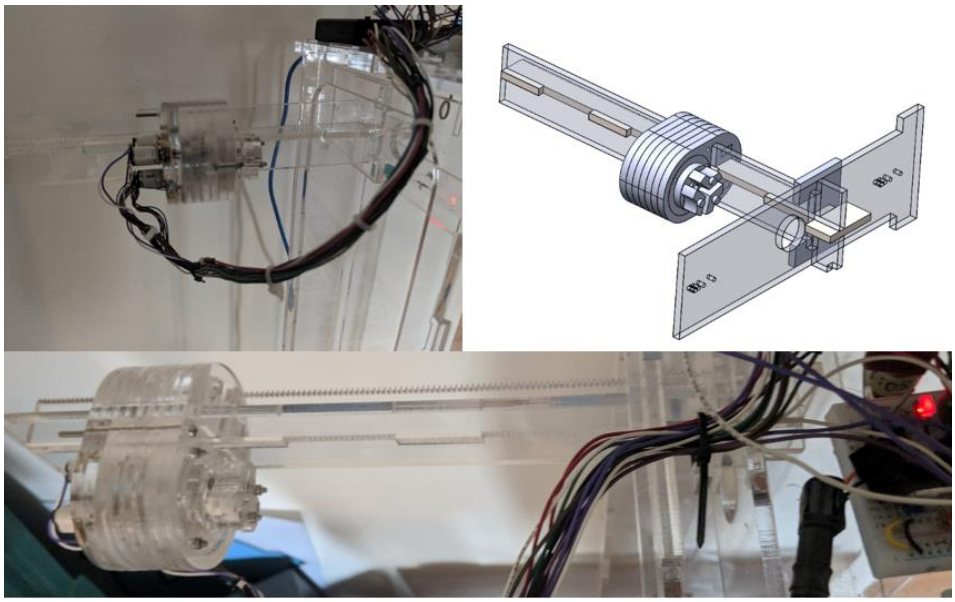

Figure 6. Rack, Track, and Coiling Machine Assembly. The Coiling Machine fit into the existing Twisting Machine. The 12” rack consists of 124 teeth. The chuck rotates and moves away from the twisting machine simultaneously

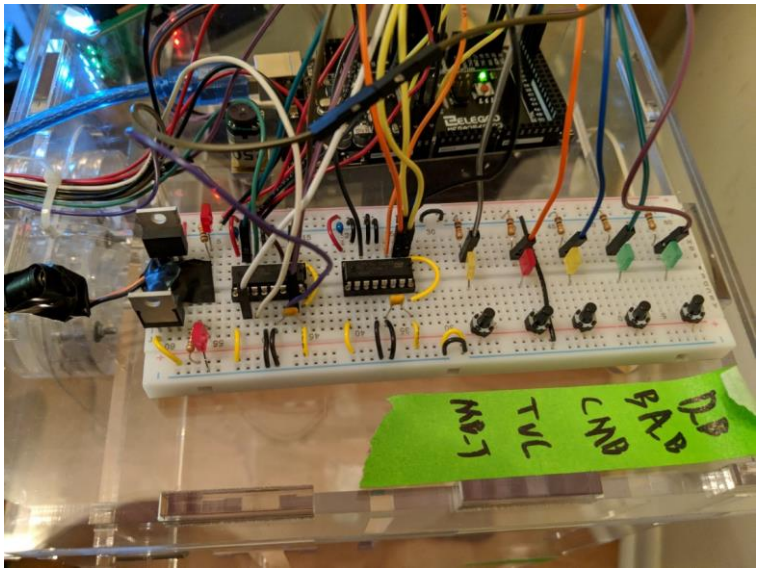

Figure 7. Control Interface. The control interface of the TCP Machine consists of a button to initiate and end twisting, a button to switch between twisting and coiling, a button to select the desired bias angle, a button to select the desired mandrel diameter, a button to imitate coiling, and an LCD screen that issues commands and requests input

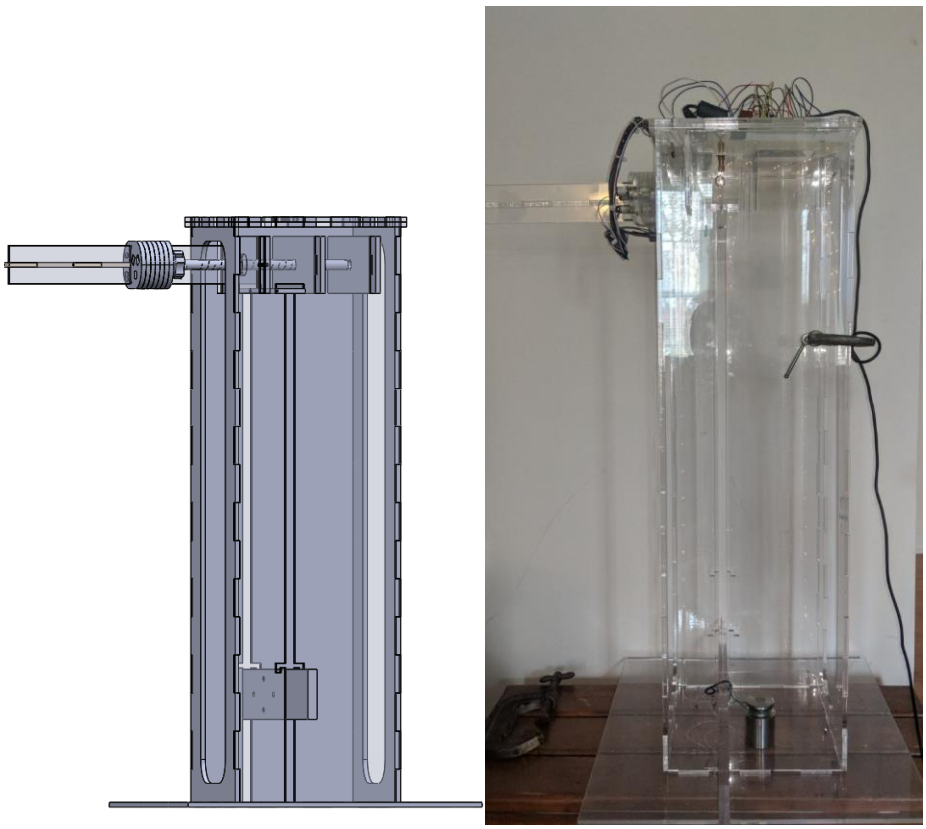

Figure 8. Full View of TCP Machine. The complete TCP machine design to the left and the fully assembled TCP machine to the right.

Annealing and Twist Setting

Annealing allows existing stresses to cohesively spread throughout a material by partially melting existing crystal structures into an amorphous phase. This heating process takes place between the polymer's glass transition and melting temperature, so that the structural shape is not altered significantly. Upon cooling the once stressed plastics have a higher percent crystallinity than before the annealing process and the reconstituted crystalline structure is aligned to the stresses that were exerted.

Despite annealing settings not being a primary focus of this research there is evidence that they are crucial for setting a fiber's shape and can drastically alter its material properties. A paper written by Kenan Yildirim in 2014 about twist setting states that an hour or more at temperatures between glass transition temperature (Tg) and melting temperature (Tm) is necessary for proper crystallization of twisted polymers; however, the same paper illustrated that thermal shrinkage post heat setting is maximized around 85 °C at 30 min for PET [15].

Since the amount of axial thermal shrinkage is a small factor that contributes to the contraction of mandrel formed TCP muscles and cannot be compared with previous research, it is a factor that was to be kept constant and not modulated in this study. Nylon 6 was heatset at 149 °C and PET was heatset at 177 °C. All plastics will be held at their desired temperature for 2 hours. These settings are consistent with those used in previous research of TCP muscles and with industry standards for annealing [16,17].

Controlled Dynamic Heating and Measuring Methodology

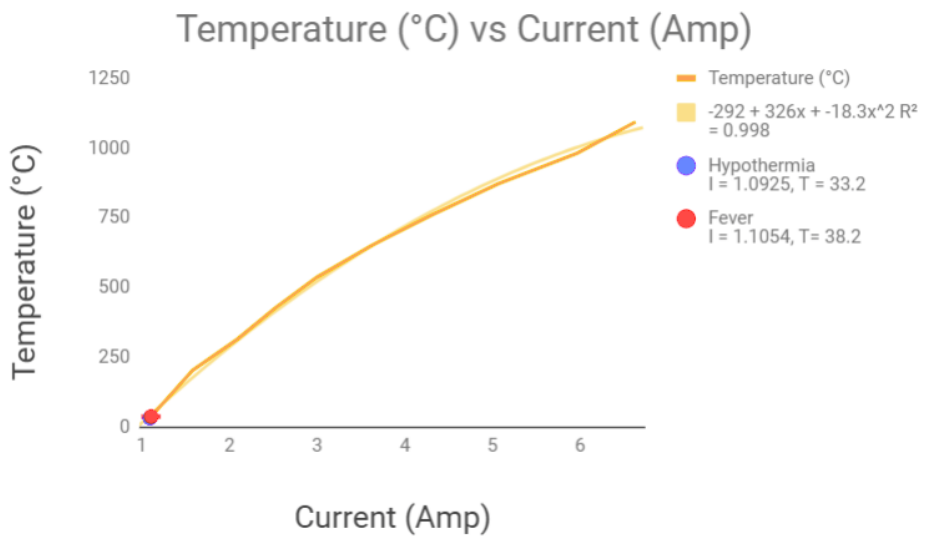

Figure 9. Temperature (°C) vs Current (Amp). For 26 gage NiCr 80 Wire $\boldsymbol{Temperature}(°\mathbf{C}) = \mathbf{-292 + 326}\boldsymbol{I}\mathbf{ - 18.3}\boldsymbol{I}\mathbf{\text{^}2}$ with a correlation coefficient of 0.998. This is an extremely good fit.

From the table listed in Wikipedia for 26 gage NiCr 80 wire Figure 12 was made. While Wikipedia is often not the best source of information, very few credible or complete sources are easily accessible for making a heating element out of NiCr wire because vaping forums and DIY community growing rapidly. The fit is very good with $R^2 = 0.998$, so in using it to determine the current and voltage required to heat the NiCr wire to specific temperatures.

The resistance of a NiCr is determined by its length. For 26 gage NiCr wire, this value is approximately 2.75 ohms/ft. From Figure 12, it is predicted that 33.2 °C corresponds to a current of 1.09A and 38.2 °C corresponds to 1.11A. To limit the voltage required by the circuit two 21" wires were run parallel to each other. These wires have a resistance of approximately 4.81 ohms.

With this data it was determined that pulse width modulation should be used to alter voltage over the NiCr wire between 5.25V and 5.33V. With a 12V 3.3A power source very little could be done to alter the voltage via voltage dividers, so an h-bridge is used to switch the sink of the NiCr wire between 3.3V and 5V. The wire has a 9V source, so it has a voltage range of 4V-5.7V. It is predicted that to achieve 33.2 °C the current should be 1.09A, the voltage should be 5.26V, and the Pulse Width Modulation (PWM) % should be 74.11%. It is also predicted that to achieve 38.2 °C the current should be 1.11A, the voltage should be 5.32V, and the PWM % should be 77.77%.

A rudimentary experiment, where the temperature was physically felt by a researcher, was done to determine if the voltages and currents were realistic. The results of this experiment determined that 5.25V felt similar in temperature to a very cold person and 5.33V felt similar in temperature to a feverish person. The circuit was neither powered nor closed during this experiment. One major issue with this design is that many instrumentation voltage regulators and wires do not function correctly with large currents, so this rig should likely use several instrumentation wires and better voltage regulators to control the current flowing through each NiCr wire.

Isotonic Testing

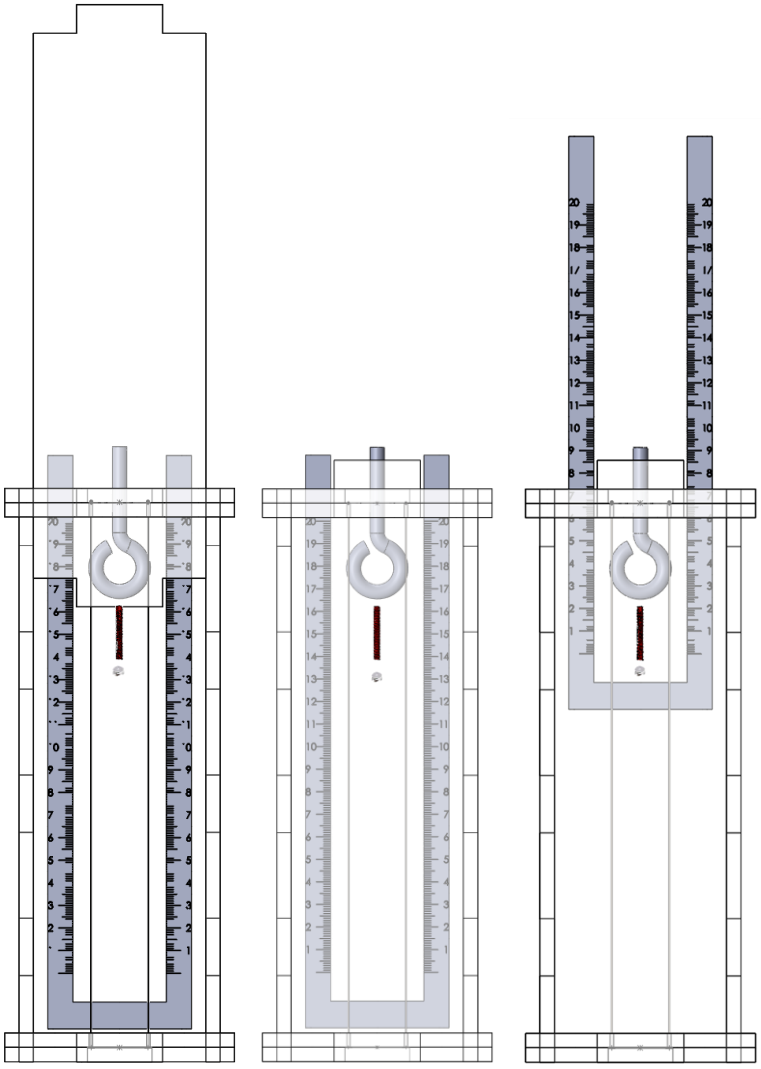

Figure 10. Isotonic Heating and Measuring Rig. The setup intended for use during constant force/stress and variable length experiments of the TCP muscles. These muscles were to be actuated over body temperature range

Figure 11. Actual Isotonic Rig. The NiCr wire was tensioned with a pair of needle-nose pliers.

The acrylic ruler worked far less efficiently than anticipated as it caught at specific angles

Isometric Testing

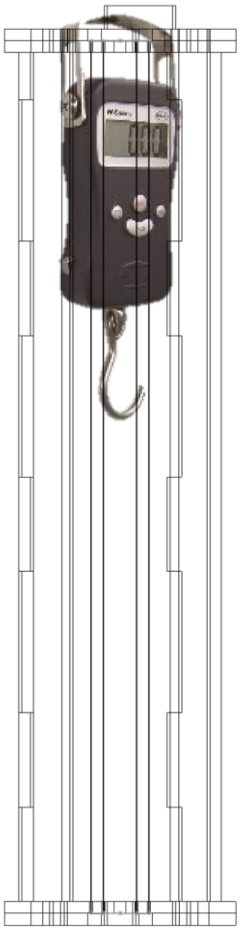

Figure 12. Isometric Heating and Measuring Rig. The proposed design of the isometric testing rig

The TCP muscles, which contact 40% or more under 0.35 MPa tension in the human body temperature range, should be further analyzed to determine their safety. An isometric experiment keeps the muscle's length constant, while it exerts a TS against an immovable object. This

experiment determines the maximum TS a muscle could exert at specific lengths and temperatures. It also determines if TCP muscles could fail catastrophically in these situations. For the purpose of safety and efficacy, both the maximum TS and failure mechanics should be understood for all possible situations; however, this experiment was not done during this research.

Fatigue Testing

Material properties of the TCP muscles, which contact 40% or more under 0.35 MPa tension in the human body temperature range and are safe to actuate, are tested with a static loading test to determine the yield and ultimate stress. To determine the lifespan of this material, the TCP muscles undergo an isotonic fatigue test at 7.5Hz while lifting a weight exerting 0.4 MPa of force. After the fatigue test, optical microscopy will be used to observe any defects that might have accrued.

Results

Monomer Characteristics

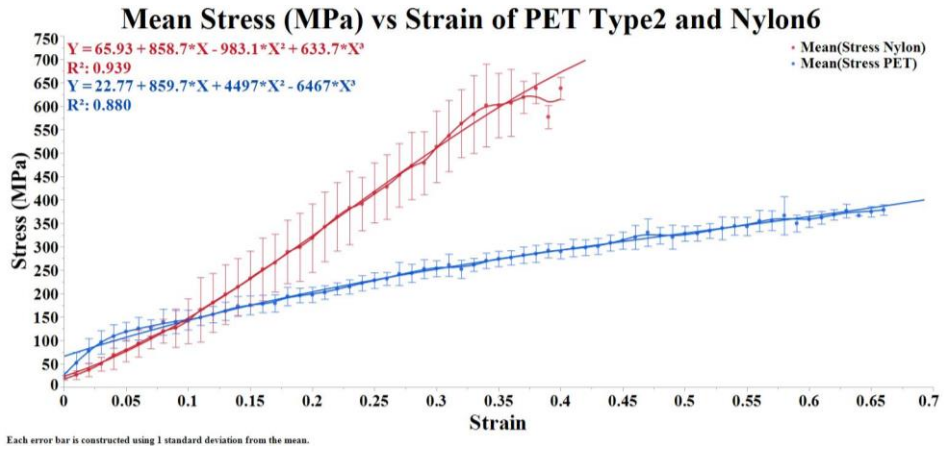

Figure 13. Mean Stress vs Strain Curve of PET Type2 and Nylon 6.

The portions of the graph in red illustrate the Stress/Strain Curve of Nylon6 and its fitted equation. The portions of the graph in blue illustrate the Stress/Strain Curve of PET Type2 and its fitted equation.

Twist Insertion

The "untwist" of a TCP muscles is directly responsible for their huge strokes. When the diameter of the coil is assumed to be constant, the change in coil length can be determined by the equation 1 below [4].

$$\Delta l_c = {l_f}^2 \Delta T / N \quad \textbf{[1]}$$

Δl_c = change in coil length

l_f = is length of filament

ΔT = change in coils/fiber length or "untwist"

N = number of coils

Equation 1 assumes that coil diameter, fiber length, and number of coils remains constant during contraction. However when a homochiral TCP muscle is heated, it contracts in length, its fiber diameter expands, and the number of coils increases slightly. During the experimentation used to create figure 14, it was observed that fiber length decreases during twist insertion even if there is no coil formation. The length change caused during heating is not well understood thermomechanically and likely has much to do with how the twist is inserted. Coil diameter does remain fairly constant until inter-coil contact occurs, but once coils do contact the diameter of the coil must be increased to fit more coils/m.

The mechanism for this untwist (ΔT) is not fully understood, but certain factors that affect the amount of initial twist can be gleaned from the equations below. The first of which dictates the torque needed for each twist-induced coil and the relative potential energy stored in the fiber. Twist-induced coiling is also known as kinking, hockling, and in the case of failure buckling. The minimum torque (τ_C) required to cause twist-induced coiling of a fiber with sufficient slack is described in the equation 2 below [12,13].

$$\tau_C = \sqrt{2EIF} \quad \textbf{[2]}$$

τ_C = torque

E = elastic modulus (MPa)

I = second moment of area = $\frac{\pi D^4}{64}$ **not** $\pi D^4/16$

F = Force = $\sigma A = \frac{\sigma \pi D^4}{4}$ **not** $4\sigma\pi D^4$

The torsion equation below relates torque to the circular fiber's shear modulus, length, and amount of turn in radians.

Commented [LU1]: site

$$\tau_C = JG\varphi/l_f \quad \textbf{[3]}$$

l_f = length of fiber

φ = radians of turn

J = torsion constant = $\pi D^4/32$

Commented [LU2]: polar moment of inertia same

G = shear modulus (MPa)

Equation 4 below reorganizes and combines equations 2 and 3 to determine the minimum twists/m needed to cause twist induced coiling for a fiber of sufficient slack (tension free line) to form a coil [12,13]. However the twisting methodology employed prevents twist-induced coiling from occurring in most situations, as there is not enough slack and/or the process of coil nucleation would not release enough torsional energy to raise a weight by a height equal to the length of the coil, $\pi D/cos(\alpha_C)$.

$$T_f = \tau_C/(2\pi JG) \quad \textbf{[4]}$$

T_f = $\frac{\varphi}{2\pi l_f}$ = Twist/m to cause twist-induced coiling

$$T_f = \sqrt{2\sigma E}/(\pi dG) \textbf{ not } 8\sqrt{2\sigma E}/(\pi dG) \quad \textbf{[5]}$$

σ= tensile stress = Force/Area

d = fiber Diameter

G = fiber shear modulus

When experimentally determining the maximum T_f for the Nylon 6 and PET of 0.25mm diameter, the only value that needs to be experimentally modulated according to Equation 5 is the tensile stress as all other factors are considered to be material constants. For this reason and to confirm the material is as the manufacturer specified, a static loading test was done to determine the ultimate stress and the stress/strain curve. From a materials property perspective, PET is the ideal material for inserting multiple twists as it has a very low shear modulus and moderate elastic modulus, so this paper compares it with Nylon 6, which has been used in published literature. This sort of experiment has not been conducted before for tensioned monofilament elastomers, so the comparison of measured results to the equation listed above is novel, so it is understandable that the errors mentioned in equations 2 and 5 were not caught in the initial publication "A New Twist On Artificial Muscles" by Haines in 2016. This equation does also illustrate the mechanism of untwist as all the number of twists inserted on a fiber would decrease as the fibers diameter increased as it heated. From these two inferences it is reasonable to think that more twists per meter and thermal expansion anisotropy, in which the fiber contracts a large amount axially and expands a large amount radially would relate directly to more contraction of the TCP muscles.

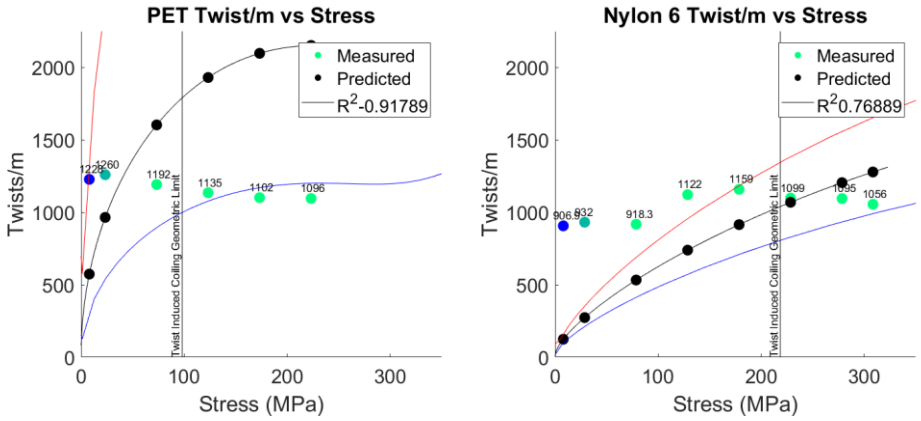

Figure 14. Twist/m vs Stress for PET and Nylon 6. There was no relation between the predicted twist/m and the measured twist/m for either monofilament

The measured points are the average values of 7 samples of 0.25m length 0.25mm diameter fibers for each unique stress. The black lines are the predicted values from equation 5 using the average shear moduli values published on matweb.com for each polymer. The blue lines and red lines are the values predicted using equation 5 using the maximum and minimum shear moduli published on matweb.com respectively for each polymer. While PET's maximum twist/m of 1260 is significantly larger than Nylon 6's maximum twist/m of 1159 this disparity is far smaller than

hypothesized. There is no significant correlation between these predicted values and the measured values

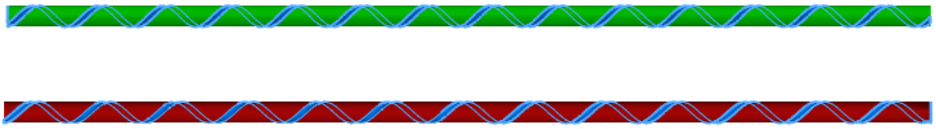

Figure 15. Illustration of the Maximum Twist PET and Nylon 6. This is an illustration of the maximum twists/m of PET in Green and of Nylon 6 in Red. For this short length of 11.21mm PET twists 14.13 times and Nylon 6 12.98 times. The blue lines are the paths of the fiber twist

The twisting machine hangs a weight fixed axially under a gear motor. This gear motor has an rpm counter and is controlled/monitored by an Arduino Mega. The number of twists is displayed on a 16x2 serial enabled LCD screen. Once the average number of twists required to cause twist-induced coiling was determined from a statistically significant sample, the motor turns only a predetermined number of times. From preliminary research, PET can take around 1260 turns/m. Nylon 6 can take around 1159 turns/m.

Coil Geometries and Their Implications

Density and Coil Bias Angle

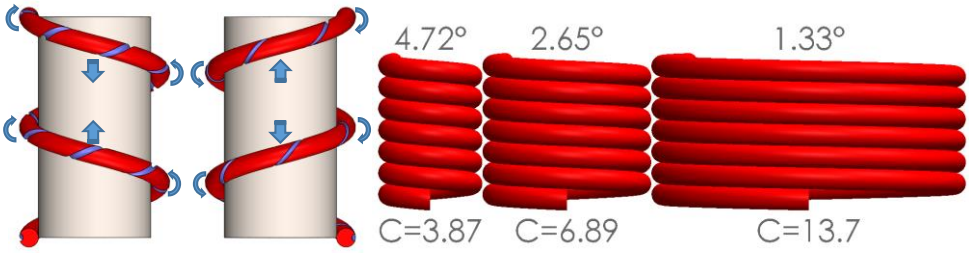

Figure 16. TCP Muscle Illustrations. The left figure is an illustration of the mechanism that actuates homochiral (left) and heterochiral (right) TCP muscles. The right figure depicts how a larger spring index fibers (coiled around larger mandrels) can contain smaller coil bias angles. Equation 14 was used to make the figure to the right

Since there is less length and more cross sectional area in a coil compared to a straight fiber, the total density does not change. However, exactly like the linear density is increased, turns per meter is also increased.

$$\text{Density} = \text{Mass}/(\text{Surface Area}*\text{Length}) \quad \textbf{[6]}$$

$$\text{Linear Density} = \text{Mass}/(\text{Length}) \quad \textbf{[7]}$$

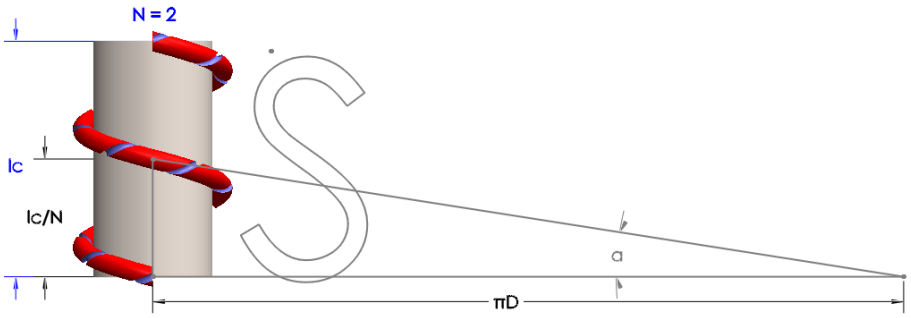

Figure 17. Coil Bias Angle Illustration. This illustration depicts a homochiral TCP muscle for a bias angle of 15° (74.12% LD Increase) and diameter of 0.068" (6.89 Spring Index). Equation 8 makes more sense when a single turn of the helix is uncoiled it forms the hypotenuse of a triangle whose adjacent leg is the circumference of the coil ($\boldsymbol{\pi D}$) and opposite leg is the distance between turns ($\boldsymbol{l_c/N}$)

Decreasing the coil bias angel (α_C) is known to increase the TC and decrease the maximum TS [4]. If the α_C is too acute, loops will come into contact and hinter further TC, while at the same time exerting large TS. For these reasons, the exact relation of coil bias angle to TC and TS is not easily defined with an equation. Coil bias angle α_C (**Fig. 7**) also physically changes the number of twists that can be inserted per meter of muscle by increasing the linear density. This angle is described by equations 8-10 below, where D is the coil diameter measured from the center of the fiber. Equation 10 is necessary when making a TCP muscle of a specific bias angle because both the distance between turns l_c/N and diameter of the coil D need to be taken into consideration.

$$sin(\alpha_c) = l_c/l_f \quad \textbf{[8]}$$

α_C = coil bias angle

l_c = length of coil

l_f = length fiber

$$cos(\alpha_c) = \pi DN/l_f \quad \textbf{[9]}$$

N = number of coils

D = diameter of coil

$$\alpha_C = tan^{-1}(\frac{l_c}{\pi DN}) \quad \textbf{[10]}$$

From equation 7 it is known that for an item of constant mass the linear density must increase the same proportion as the length decreases. Taking equation 8 and this information into account, equation 11 is formed to determine the increase in linear density only from the coil bias angle. A visualization of equation 11. Equation 12 may be unintuitive, but all coils of the same bias angle and fiber length have the same linear density regardless of their coil diameter.

$$100(1 - \sin(\alpha_C)) = \%\ \text{linear density increase} \quad \textbf{[11]}$$

$$\frac{\text{mass}}{l_f \sin(\alpha_C)} = \text{linear density} \quad \textbf{[12]}$$

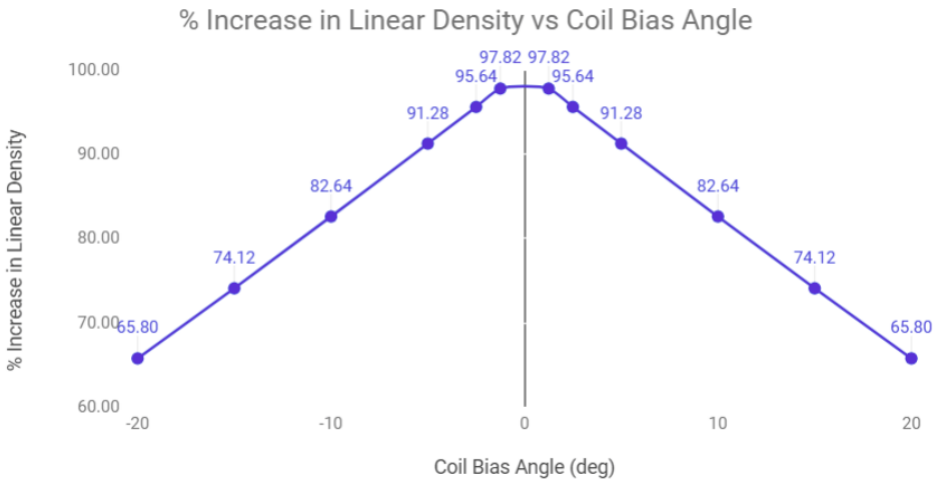

Figure 18. % Increase in Linear Density vs Coil Bias Angle. As the coil bias angle increases the linear density decreases linearly. It has been demonstrated in published literature that increasing the linear twist density of TCP muscles increases their TC [4]. The % increase in linear density is determined by equation 11 and is a purely geometrical property

Diametric Ratios and Spring Index

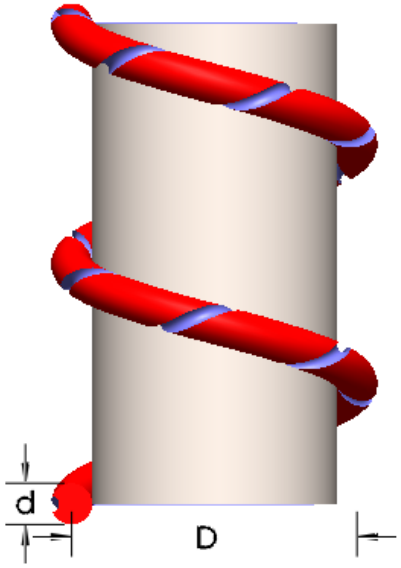

Figure 19. Diametric Ratio and Spring Index Illustration. This illustration depicts a homochiral TCP muscle for a bias angle of 15° (74.12% LD Increase) and diameter of 0.068" (6.89 Spring Index). The ratio of nominal coil diameter measured from the center of the fiber to fiber diameter is known as the spring index

Linear density is constant for regardless of coil diameter as long as α_c and fiber diameter are constant; however, coils with larger diameters can accommodate a smaller α_C **(Fig. 2)**. The spring index (C) of the coil is determined by the equation 13 below.

C = Nominal Coil Diameter/Fiber Diameter **[13]**

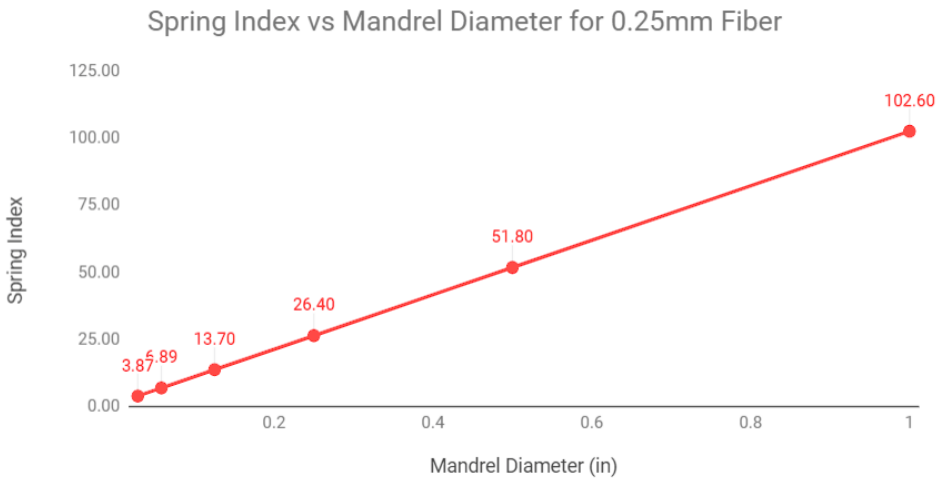

Figure 20. Spring Index vs Mandrel Diameter for 0.25mm Fiber. Coil Diameter is the mandrel diameter plus the fiber diameter. The spring index's for the muscle geometries intended by this study are illustrated above for all mandrel diameters

The spring index has an impact on how efficiently coils contract and untwist and also changes the spacing of the coils. Coils that have more than 60% of their length made up by fiber diameter will likely come into contact before contracting the required 40% in length. Coils with larger diameters are known to have larger TC and lower TS [4]. It has been theorized that these factors can be combined to tailor the properties of TCP muscles; however a comprehensive study that combines these factors has not been done [4,13,14]. This study will combine coil bias angles (α_C) of 1.25°, 2.5°, 5°,10°,15°, and 20° and spring indexes of 102.60, 50.8, 25.4, 12.7, 6.4, and 3.2 to make 36 unique data points for both TC and TS. However, because of limitations illustrated in Figure 10 only 17 of these coils can be made. The results from these experiments will be displayed on a

linearly interpolated 2D surface plot with an equation fit to it by the MATLAB function polyfitn(spring index, bias angle) = (TC, TS).

Commented [LU3]: add equation to describe which BA are not okay

Possible Geometries and Hypothesis Formation

For the pursuits of muscles which can contract more than 40% equations 14-18 can be used to rule out geometries that would have coil self-contact before this value is reached. Equation 14 describes the distance between turns in terms of diameter and coil bias angle. Equation 15 is the vertical length the each fiber takes up when coiled. Equation 16 is the point of coil contact where equation 14 is equivalent to equation 15. The minimum bias angle in radians for a coil of diameter D formed from a fiber of diameter d is defined in equation 17. Equation 18, the optimal distance between coils for a TCP muscle which contracts 40% its length before having inter-coil contact for all diametric combinations. A very good easy approximation of equation 18 or the optimal distance between turns is 40% more than the diameter of the fiber. This approximation has a maximum error of only 5.2% in the geometrically limiting case of D=d.

Commented [LU4]: let me know how you would like this formatted

Distance between turns

$$\frac{l_c}{N} = \pi D \tan(\alpha_c) \quad \textbf{[14]}$$

Vertical cross section of fiber

$$d/\cos(\alpha_c) \quad \textbf{[15]}$$

The coil of diameter D comes into contact when

$$d/\cos(\alpha_c) = \pi D \tan(\alpha_c) \quad \textbf{[16]}$$

Angle of coil contact

$$\alpha_{c_{min}} = 2 \tan^{-1}\left(\frac{\pi D - \sqrt{\pi^2 D^2 - d^2}}{d}\right) \textbf{[17]}$$

All coils that can contract by 40% have a distance between turns larger than

$$\frac{l_c}{N} = 1.4\pi D \tan(\alpha_{c_{min}}) \textbf{[18]}$$

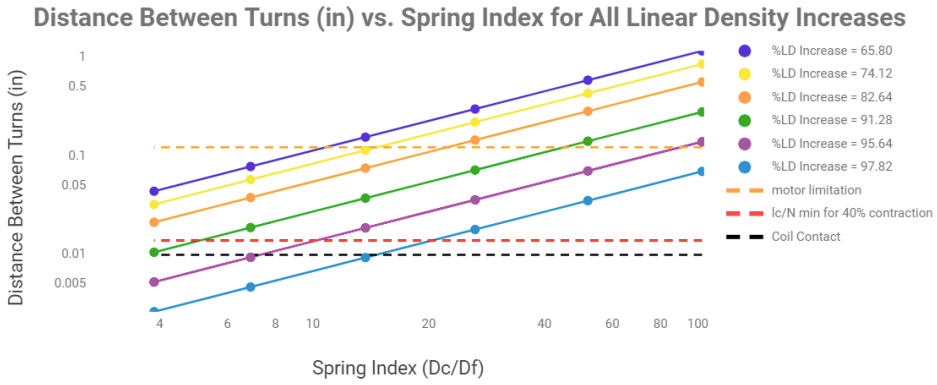

Figure 21. Distance Between Turns (in) vs. Spring Index for All Linear Density Increases.

The dashed red line is the point at which the coils would have inter-coil contact before achieving 40% contraction. The dashed black line is the point of impossible coil geometries. The dashed orange line is the point where the coiling machine motors do not work

For all 36 unique combinations of mandrel diameters and coil bias angles 5 are physically impossible, 1 is not applicable for 40% contraction, and 14 cannot be made because of motor limitations. This leaves 17 possible coil geometries. The dc motors used in the coiling machine have maximum and minimum voltage limitations in which correspond to their maximum and minimum rotations per minute. When combining the limitations of both the chuck and pinion motors, it was found that coils further apart than 0.1219" were not possible for this machine.

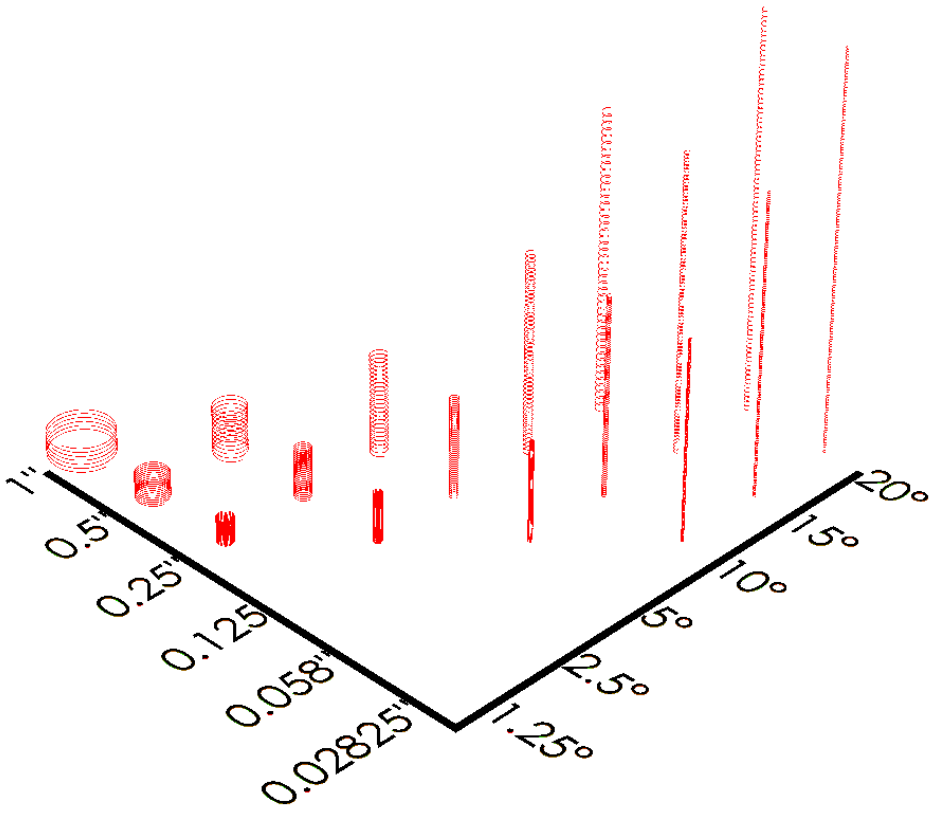

Figure 22.Illustration of the 17 Possible Coil Geometries. The underlying theory of this paper is that the coil of the smallest bias angle and largest coil diameter will contract the most and that the coil of the largest bias angle and smallest diameter will contract the least. In other words, the coil of the largest spring index and highest linear twist density will have a higher TC than the coil of the smallest spring index and lowest linear twist density

Coil Bias angle that leaves 40% of contraction without contact

$$\alpha_{c_{140\%}} = \tan^{-1}(1.4\tan(\alpha_{c_{min}})) \quad \textbf{[19]}$$

Combining equations

$$\Delta T = \frac{0.4\sin(\alpha_{c_{140\%}})\cos\left(\alpha_{c_{140\%}}\right)}{\pi D} \quad \textbf{[20]}$$

Table 1. Literature Maximum Contraction and Hypothesized Ideal Coil Geometries

	Haines 2014	Measured Literature Max	Hypothesized Literature Max	Hypothesized Coil Geometry	Hypothesized Coil Geometry
Material	Nylon 6	Nylon 6	Nylon 6	Nylon 6	Nylon 6
Mandrel Diameter (in)	0.1524	0.04429	0.04429	0.16690	0.08378
Coil Diameter (in)	0.1862	0.05413	0.05413	0.17675	0.09362
Fiber Diameter (in)	0.03386	0.009843	0.009843	0.009843	0.009843
Spring Index	5.5	5.5	5.5	17.96	9.512
Initial Coil Bias Angle (deg)	5	5	5	1.477	2.684
Final Coil Bias Angle (deg)	3.318	3.318	3.318	1.016	1.918
Initial % Linear Density Increase	91.28	91.28	91.28	97.52	95.32
Final % Linear Density Increase	94.21	94.21	94.21	98.23	96.65
Change in % Linear Density Increase	+2.928	+2.928	+2.928	+0.7087	+1.336
Temperature Min (°C)	25	25	25	33.2	33.2
Temperature Max (°C)	95	95	44.7	38.2	38.2
ΔTemperature (°C)	70	70	19.66	5.000	5.000
l_f (in)	~5.371	19.69	19.69	19.69	19.69
$l_{c_{initial}}$ (in)	~0.4681	1.716	1.716	0.4884	0.9217
$l_{c_{final}}$ (in)	~0.2387	0.8750	0.8750	0.2931	0.6588
Δl_c (in)	~0.2294	0.8407	0.8407	0.1954	0.3687
$\Delta l_c / l_c$ (in)	0.4900	0.4900	0.4900	0.4000	0.4000
N	~10.5	115.3	115.3	35.44	66.86
ΔTwist/m	~0.2502	0.2502	0.8606	0.01787	0.06361

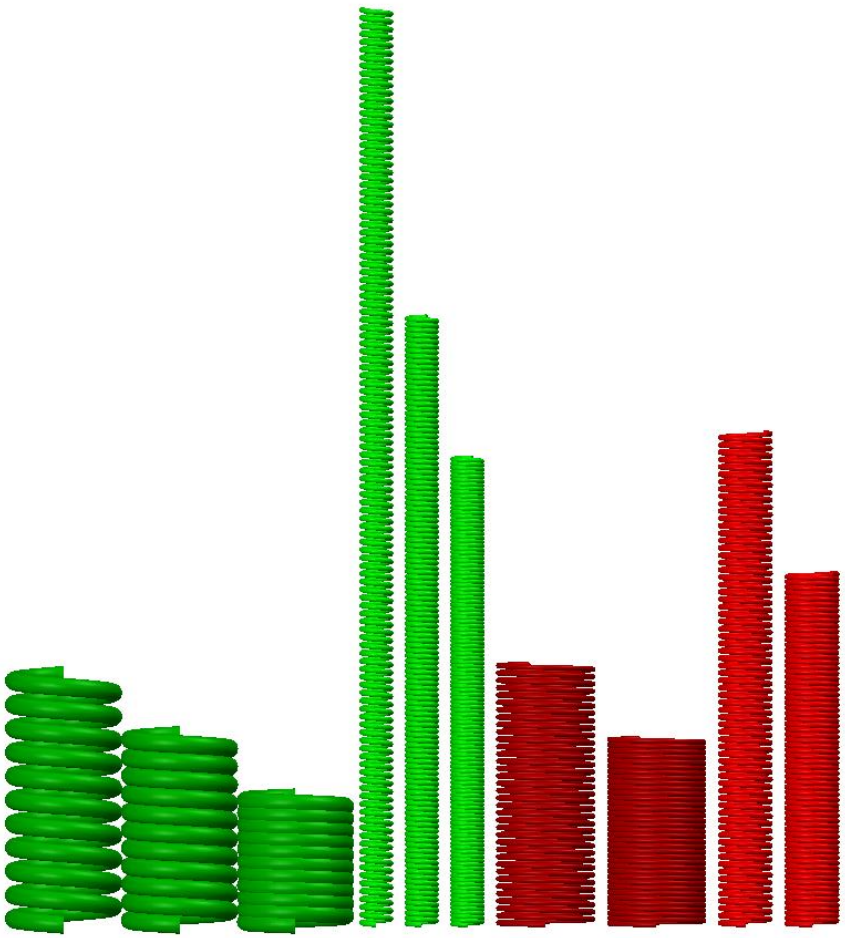

Figure 23. Literature Maximum Contraction and Hypothesized Ideal Coil Geometries. The coils in green from left to right are the initial coil geometry, the point of inter-coil contact, and the maximum contraction of a 5.5 spring index coil with 5° bias angle. The red geometries are the hypothesized geometries

It was published in Haines et al 2014 that the dark green coil geometry in figure could contract by 49% in a temperature range of 70°C. If the 0.25 Nylon 6 has the same untwist/m and geometric configuration, it would have the same LA over the same temperature range as depicted by the light green coil in figure 23. However, if the twist/m accepted by a fiber is inversely proportional to its diameter, the amount of untwist is linearly related to the amount of twist inserted, and the amount of twist inserted is increased linearly by decreasing diameter then it could have the same LA with the same geometric configuration over a temperature range of 19.663°C.

With the equations proposed in this paper the exact geometry necessary for a coil to cause contraction in human body temperature range can be predicted; however, the relation of diameter to untwist and the relation of twist insertion to diameter are not well understood. The dark red coils represents a coil made from 0.5m of 0.25mm Nylon 6 contracting 40% its length in a 5°C temperature range. This dark red coil has 5/70ths the amount of untwist as the dark green coil as it is working in a temperature range 5/70ths the amount as the dark green coil. The light red coils represents a coil made from 0.5m of 0.25mm Nylon 6 contracting 40% its length in a 5°C temperature range. This light red coil has 43/175ths the amount of untwist as the dark green coil as it is working in a temperature range 5/70ths the amount as the dark green coil and has a fiber diameter of 0.25mm while the dark green coil has a fiber diameter of 0.86mm, so the 0.25mm fiber should be able to accept 86/25x the twists per meter the 0.86mm fiber could and should be able to untwist the 86/25x the amount eh 0.86mm fiber could. While several different geometric ratios of bias angle and spring index could likely achieve these parameters, the coil geometries proposed in table 1 and illustrated in figure 23 are the densest (i.e. most space efficient) for their

desired function, but are less space efficient than TCP muscles formed by twist-induced coiling (i.e. Fig 24).

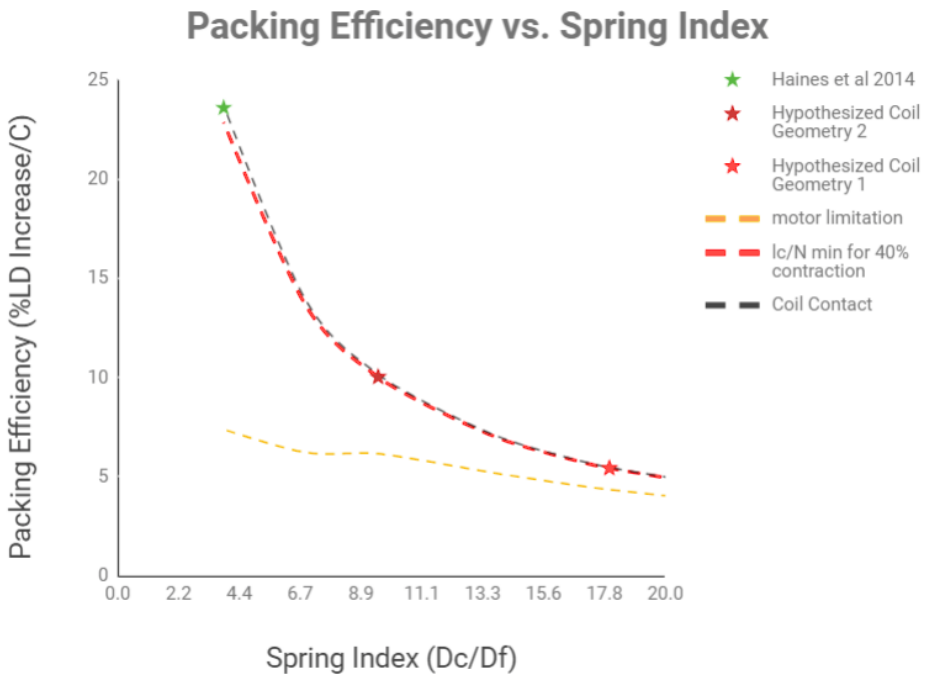

Figure 24. Packing Efficiency vs. Spring Index. The coils seen in Figure 22 described in terms of their packing efficiencies.

Summary

Discussion

The purpose of this study was to determine if a functional TCP muscle could be made to contract 40% its initial length and exert a 0.35 MPa force in a 5 °C temperature range. This question was not answered during this study and the underlying hypothesis that more linearly dense coils of larger spring indices will contract more than less linearly dense coils of smaller spring indices was never tested, as no mandrel formed coils could be made by the researchers. The process of twisting and coiling is challenging and should be carefully described in all future publications to improve the reproducibility of results.

While twisting may seem like a rudimentary task, maximization of a monomer's twist/m is best done using short lengths of monomers and stresses above the yield point. This makes hanging a weight under a long fiber both impractical and disadvantageous. In order to both twist and coil, the twisting of the fiber should either be done very close to the mandrel or should be done at a short distance between one spool and another that will later unspool onto the mandrel.

Access to several facilities that could be used in lieu of the several machines designed for this experiment as an automated lathe or textile twisting/spooling machine would accomplish TCP muscle manufacturing easily. A precision heating machine, such as a tube furnace, would be instrumental for quickly and precisely actuating temperature changes required by the isotonic, isometric, and fatigue tests. The creation of both of these machines by the researcher was time consuming and prevented the experiment from progressing past twist insertion.

During this research, the equation proposed by Haines et al in 2014 was analyzed and was contradicted by the results in this paper. The most space efficient geometric configurations that

should allow contraction of 40% were predicted assuming that the fiber untwist was controlled by its diametric change and is truly responsible for the large TC of TCP muscles. From this experimentation it was observed that the coil geometry previously proposed in Haines et al employed the same geometric parameters that would allow it to contract 40% without inter-coil contact regardless of what tensile stress it is under. This confirms the theory behind the ideal coil geometries proposed in this paper.

Future Directions

TCP Muscles have applications beyond their demonstrated utility as external prosthetic limb actuators [5,6,7,8,9]. The characteristics of these muscles are only material and geometry based, so they are uniquely scalable to any desired size [4,13,14,16]. The materials used in this project are known biomaterials already approved for applications within the human body [15,16]. These two properties allow TCP Muscles to be applicable for implantable synthetic muscles, biodegradable in vivo bioreactors, and surgical nanomachines.

TCP muscles have proven that they can actuate loads of heavier than 0.35 MPa by more than 40% their initial length [4]. If they could do the same task within body temperature range of 33°C to 38°C, the temperature change caused by existing muscle activation could be used to actuate the TCP Muscles leading towards body powered exoskeletons and chronically implanted assistive devices. The lowered temperature range could also allow for faster contraction, lower contraction energy, and elastocaloric cooling caused by the contraction of antagonist muscles. The efficiency of these muscles could even be used for better mechanical contraction of modern day machinery. The broad potential applications of these muscles are promising, but research has not yet been able

to make the temperature ranges needed to actuate them reasonable as the relation of certain fabrication parameters to TS and TC is not yet known [4,13,14,16].

The future aims that should be accomplished are in relation to twist insertion scaling and coil geometries. The first aim of fully understanding twist insertion should be accomplished with a 4 dimensional analysis of twist insertion where fiber diameter and fiber length are independent variables. The dependent variables should be twists/m and the fiber's end length. The second aim of understanding the impact of coil geometries should be met with 4 dimensional analysis where spring index and coil bias angel are independent variables and TC is a dependent variable, while twist/m and TS are held constant. When these aims are met the viability and characteristics of TCP muscles can be fully analyzed.

Some future design considerations are the annealing settings and their effect on TS and TC, scalability of TCP muscles, packing efficiency and its relation to TS and TC, the effects of braiding and bundling parameters on TS and TC, the possibility of TCP muscle braids or bundles to be twisted and coiled to alter TS and/or TC, pairing homochiral and heterochiral muscles to account for length changes caused by ambient temperature fluctuation, and the amount elastocaloric cooling that occurs in different situations.

Conclusion

While the main aim of this research was not to determine the stress needed to insert the maximum number of twists into Nylon 6, Nylon 6/6, and PET, it is the primary result and the hypotheses used to predict the optimal material for twist insertion were disproven. The primary aim was to

understand and quantify the relationship of spring index and coil bias angle to TS and TC; however, this goal was unattainable because of time constraints and several project setbacks. With these factors quantified in relation to TS and TC it was hypothesized that a specific combinations of manufacturing settings will create viable synthetic muscles, which actuate within the range of human body temperature. Additional research should be done to determine if multiple annealing sessions could allow more twist/m, the impacts that different braiding settings have on TC and TS, and if twisting and coiling braided or bundled TCP muscles improves their TS and TC qualities.

Acknowledgements

Sarah Steele Danhoff Undergraduate Research Award for funding

Bryan Labra for assisting with experiment

Dr. Kenneth Donnelly for discussing broad scope of research and advising

Dr. Naji Husseini for discussing material properties

Dr. Tushar Ghosh for discussing manufacturing methodologies

Yuanqi Li at TORAY MONOFILAMENT CO., LTD. for supplying the samples of PET

Dr. Ray Baughman and Carter Haines of the NanoTech Institute at the University of Texas in Dallas

Dr. Claudio Battaglini and and Dr. Claudio Battaglini for discussing muscle characteristics

References

1. Iezzoni LI, McCarthy EP, Davis RB, Siebens H. (2001). Mobility Difficulties Are Not Only a Problem of Old Age. Journal of General Internal Medicine. 16(4):235-243. doi: 10.1046/j.15251497.2001.016004235
2. I. Hunter & S. Lafontaine, (1992). A comparison of muscle with artificiall acutators. Technical Digest IEEEE Solid State Sensors & Actuators Workshop, 178-185.
3. J. D. W. Madden et al., (2004). IEEE J. Oceanic Eng. 29 , 706–728.
4. Carter S. Haines, et al., (2014). Artificial muscles from fishing line and sewing thread. Science, 343, 868–72. doi: 10.1126/science.1246906
5. Wu, L., et al. (2017). Compact and low-cost humanoid hand powered by nylon artificial muscles.Bioinspiration & Biomimetics. 12(2): p. 026004.
6. Saharan, L., et al. (2017). Design of a 3D printed lightweight orthotic device based on twisted and coiled polymer muscle: iGrab hand orthosis. in SPIE Smart Structures and Materials+ Nondestructive Evaluation and Health Monitoring. International Society for Optics and Photonics.
7. Saharan, L., Andrade, M. J., Saleem, W., Baughman, R. H., & Tadesse, Y. (2017). IGrab: hand orthosis powered by twisted and coiled polymer muscles. Smart Materials and Structures, 26(10), 105048. doi:10.1088/1361-665x/aa8929
8. Tadesse Y, Wu L and Saharan L K. (2016). Musculoskeletal system of bio-inspired robotic systems Mech. Eng.138 S11–15
9. Saharan, L., & Tadesse, Y. (2016). Robotic hand with locking mechanism using TCP muscles for applications in prosthetic hand and humanoids. Bioinspiration, Biomimetics, and Bioreplication 2016. doi:10.1117/12.2219535

10. S. Das, S. J. Hollister, C. Flanagan, A. Adewunmi, K. Bark, C. Chen, K. Ramaswamy, D. Rose, E. Widjaja, (2003) "Freeform fabrication of Nylon-6 tissue engineering scaffolds", Rapid Prototyping Journal, vol. 9, no. 1, pp.43-49.
11. H. Seitz, S. Marlovits, I. Schwendenwein, E. Müller, and V. Vécsei. (1997).“ Biocompatibility of polyethylene terephthalate (Trevira® hochfest) augmentation device in repair of the anterior cruciate ligament,” BIOMATERIALS, vol. 19, pp. 189-196.
12. Carter S. Haines, Na Li, Geoffrey M. Spinks, Ali E. Aliev, Jiangtao Di, and Ray H. Baughman. (2016). New twist on artificial muscles. PNAS, 113(42), 11709-11716.
13. Ross AL. (1977) Cable kinking analysis and prevention. J Eng Ind 99(1):112–115.
14. Aziz, Shazed Md. (2017). Polymer Fibre Artificial Muscle, Doctor of Philosophy thesis, School of Mechanical, Materials, Mechatronic and Biomedical Engineering, University of Wollongong.
15. Yildirim K and Ulcay Y. (2014). An experimental study and model development of poly(ethylene terephtalate) yarn Morphology. e-Polymer. 14: 121–131.
16. Saharan, L., & Tadesse, Y. (n.d.). Conference Paper Full-text available Fabrication Parameters and Performance Relationship of Twisted and Coiled Polymer Muscles. ASME 2016 International Mechanical Engineering Congress and Exposition. doi:10.1115/IMECE2016-67314
17. Materials Engineering. (2013, August 01). Retrieved December 21, 2017, from http://www.substech.com/dokuwiki/doku.php?id=annealing_of_plastics